Available online at www.sciencedirect.com
SCIENCE DIRECT
Journal of Sound and Vibration 264 (2003) 433–451
JOURNAL OF SOUND AND VIBRATION
www.elsevier.com/locate/jsvi

The quantification of structure-borne transmission paths by inverse methods. Part 2: Use of regularization techniques

A.N. Thite, D.J. Thompson*

Institute of Sound and Vibration Research, University of Southampton, Highfield, Southampton SO17 1BJ, UK

Received 28 August 2001; accepted 20 June 2002

Abstract

The inversion of an ill-conditioned matrix of measured data lies at the heart of procedures for the quantification of structure-borne sources and transmission paths. In an earlier paper the use of over-determination, singular value decomposition and the rejection of small singular values was discussed. In the present paper alternative techniques for regularizing the matrix inversion are considered. Such techniques have been used in the field of digital image processing and more recently in relation to nearfield acoustic holography. The application to structure-borne sound transmission involves matrices, which vary much more with frequency and from one element to another. In this study Tikhonov regularization is used with the ordinary cross-validation method for selecting the regularization parameter. An iterative inversion technique is also studied. Here a form of cross-validation is developed allowing an optimum value of the iteration parameter to be selected. Simulations are carried out using a rectangular plate structure to assess the relative merits of these techniques. Experiments are also performed to validate the results. Both techniques are found to give considerably improved results compared to singular value rejection.

1. Introduction

Transfer path analysis is an experimental technique for quantifying the contribution from different paths to the noise at a receiver position. It is widely used in the automotive industry, for instance Ref. [1–4]. In transfer path analysis, forces are usually identified indirectly from an accelerance matrix and a set of operational accelerations. At each frequency a matrix inversion is required. The measurements of accelerances from source locations to the response locations and operational responses, measured at a series of locations due to the operational source, however,

*Corresponding author. Tel.: +44-23-8059-2510; fax: +44-23-8059-3190.
E-mail address: djt@isvr.soton.ac.uk (D.J. Thompson).

PII: S0022-460X(02)01203-8

involve errors. These are magnified by the matrix inversion, particularly at frequencies where the condition number of the accelerance matrix is high [5–8]. This ultimately leads to errors in estimates of the contributions from these forces via different paths to the response. Hence, it is important that the forces are identified reliably for the analysis to produce reliable results.

The force identification errors can generally be reduced by over-determination, i.e., using a larger number of responses than the forces to be identified, and employing a least-squared error solution given by Moore–Penrose pseudo-inversion. In such a solution, however, it is observed that the errors in force reconstruction continue to be large at frequencies where the accelerance matrix is ill conditioned [5,9]. This can, for example, be due to the fact that only a small number of modes contribute significantly to the operational responses close to resonances; this number can be smaller than the number of forces to be identified [10,11].

The least-squares solution can also be achieved through singular value decomposition of the accelerance matrix. It is possible in this case to discard insignificant singular values in order to improve the effective condition number of the accelerance matrix and hence improve the force identification. To discard singular values a threshold is required. This can be based on an estimate of the error in the measured accelerances [5] or the error in the measured operational accelerations [8]. As seen in the companion paper [11], however, singular value rejection does not overcome the large force reconstruction error in the vicinity of antiresonance and the individual contribution from each force may contain large errors when a small number of modes (less than the number of forces) are contributing to the responses, even though the overall response might be correct. Moreover, singular value rejection can induce an under-prediction of the response due to the loss of information.

For a long time in the field of digital image processing and more recently in relation to nearfield acoustic holography (NAH), other techniques have been employed to improve source reconstruction [12–16]. These include Tikhonov regularization and iterative inversion techniques. In these techniques, instead of minimizing a cost function based on ordinary least-squared errors, a function which incorporates some bias is introduced. This new function is minimized to identify the source. In both techniques, the error in the force reconstruction is divided into a bias error and a magnified variance. In the ordinary least-squares solution only the magnified variance is present and no bias error is introduced. There can be a large magnification of the variance at frequencies where the accelerance matrix is ill conditioned. By introducing a bias error which increases with the value of a regularization parameter, it is observed that there exists a point (value of regularization parameter or number of iterations) where the bias error and the random error cross over. For iterative inversion of the (5×4) accelerance matrix considered in this paper at one of the frequencies a typical variation of bias error and variance is shown in Fig. 1. For smaller iteration numbers the bias error dominates, for larger values the random error dominates. For an infinite number of iterations the bias tends to zero and the random error tends to that in the Moore–Penrose pseudo-inverse. Near the cross-over point the cost function is minimized. The introduction of a bias error limits the magnification of random errors in the accelerance and the operational responses. This comes, however, at the cost of a small bias error in the force reconstruction. A similar result applies to Tikhonov regularization.

In this study the use of Tikhonov regularization and iterative inversion is investigated in a numerical simulation of a transfer path analysis application in which the test object is a rectangular simply supported flat plate [11]. Four simultaneous coherent broadband forces are

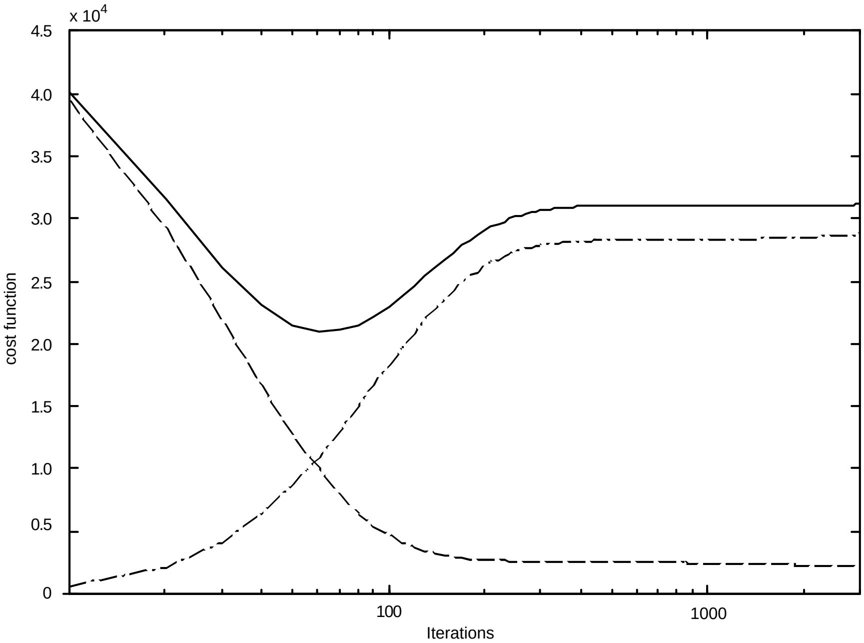

Fig. 1. Example of the bias error and variance as function of number of iterations for the iterative inversion of 5×4 analytical accelerance matrix with noise at 70 Hz: – – – – , bias; —· — · — , variance; and ——— , total error.

considered and five responses are used to reconstruct them. Although this structure is the same as in the companion paper [11], the assumed noise levels in the measurements are consistently greater in order to give increased discrimination between the methods. Results should, therefore, not be compared directly between the two papers. However, some tabulated results for the earlier methods are included, derived using the present data. The findings from the numerical simulations are also validated by experimental inverse force identification.

2. Tikhonov regularization

2.1. Method

The ordinary least-squares solution for the inverse problem (force identification) generally results in large force reconstruction errors at frequencies where the accelerance matrix has a high condition number. Under such circumstances, it is possible to improve the reconstruction by 'regularizing' the solution. One type of regularization which has already been studied [11] is singular value rejection based on the error norm. Other regularization methods are based on the introduction of bias in the solution. This is explained below, which follows [13–15,17], though here applied to the structural case.

At each frequency the vector of observed operational responses (accelerations) $\hat{\mathbf{a}}$ can be represented as

$$\hat{\mathbf{a}} = \mathbf{a} + \mathbf{e}, \tag{1}$$

where $\mathbf{a}$ is the true response and $\mathbf{e}$ is the measurement error vector. This expression can also be written as

$$\hat{\mathbf{a}} = \mathbf{AF} + \mathbf{e}, \tag{2}$$

where $\mathbf{A}$ is the matrix of theoretical accelerances and $\mathbf{F}$ is the true force vector, assuming that all forces are accounted for. However, an additional error $\tilde{\mathbf{e}}$ can be identified, that is due to the matrix inversion. The reconstructed forces $\hat{\mathbf{F}}$ can be used with the measured FRF matrix, $\hat{\mathbf{A}}$ to calculate the operational responses

$$\tilde{\mathbf{a}} = \hat{\mathbf{A}}\hat{\mathbf{F}} + \tilde{\mathbf{e}}. \tag{3}$$

The least-squares solution (e.g., the Moore–Penrose pseudo-inverse) aims to determine $\hat{\mathbf{F}}$ such that the fitting errors $\tilde{\mathbf{e}}$ are minimized, i.e.,min$(\tilde{\mathbf{e}}^{\mathrm{H}}\tilde{\mathbf{e}})$ where H indicates Hermitian transpose. These fitting errors may come from errors in $\hat{\mathbf{A}}$, in $\hat{\mathbf{a}}$ or in the model used (e.g., additional inputs). Instead of the ordinary least-squares solution, Tikhonov suggested [18] minimizing a cost function given by

$$J = \min\{(\tilde{\mathbf{e}}^{\mathrm{H}}\tilde{\mathbf{e}}) + \lambda(\hat{\mathbf{F}}^{\mathrm{H}}\hat{\mathbf{F}})\}, \tag{4}$$

where λ is a regularization parameter to be determined. This cost function introduces a bias into the solution which can be adjusted (by varying λ) to limit the magnification of measurement errors due to ill conditioning. The minimization of the cost function results in the following expression for the identified forces:

$$\hat{\mathbf{F}} = (\hat{\mathbf{A}}^{\mathrm{H}}\hat{\mathbf{A}} + \mathbf{I}\lambda)^{-1}\hat{\mathbf{A}}^{\mathrm{H}}\hat{\mathbf{a}}. \tag{5}$$

Eq. (5) can also be written in terms of the singular values of the accelerance matrix, which can be decomposed as $\hat{\mathbf{A}} = \mathbf{USV}^{\mathrm{H}}$, with $\mathbf{U}$ and $\mathbf{V}$ unitary matrices and $\mathbf{S}$ a diagonal matrix of singular values s_i. This gives

$$\hat{\mathbf{F}} = \mathbf{V}(\mathbf{S}^{\mathrm{T}}\mathbf{S} + \mathbf{I}\lambda)^{-1}\mathbf{S}^{\mathrm{T}}\mathbf{U}^{\mathrm{H}}\hat{\mathbf{a}}. \tag{6}$$

This can be compared with the pseudo-inversion in which $\hat{\mathbf{F}} = \mathbf{VS}^{-1}\mathbf{U}^{\mathrm{H}}\hat{\mathbf{a}}$ [11]. In Eq. (6) the term $(\mathbf{S}^{\mathrm{T}}\mathbf{S} + \mathbf{I}\lambda)^{-1}\mathbf{S}^{\mathrm{T}}$ is a diagonal matrix having elements $s_i/(s_i^2 + \lambda)$, which replaces the usual $\mathbf{S}^{-1}$, the terms of which are s_i^{-1}.

As can be seen from the above relation, the regularization parameter effectively modifies the singular values in the inverse. In doing this it introduces a bias error into the solution. When the condition number of the accelerance matrix is high, the effect of smaller singular values, which are prone to errors, can be nullified by choosing an appropriate regularization value λ. The effect of adding an optimal regularization parameter to larger singular values results in a small bias. However, it is essential to choose a proper regularization value so that it results in minimum magnification of measurement errors while introducing negligible bias into the solution. To do this, it is necessary to know the errors in the measurements, or to use mathematical methods which approximate them, in order to find the optimal regularization parameter. One of the mathematical concepts to choose regularization parameters when errors in the measurement are not known is explained below.

2.2. Ordinary cross-validation

The method of ordinary cross-validation was suggested by Allen [19]. In this method, out of m responses only $(m-1)$ are used initially in the force identification. The forces so identified are then used to reconstruct the remaining response. This can be done for different values of regularization parameter. The closeness of reconstruction of this response indicates the effectiveness of the chosen regularization parameter.

Writing the identified forces with the kth element of the response left out as $\hat{\mathbf{F}}_k$, etc., the square of the deviation is $|\hat{\mathbf{a}}_k - \hat{\mathbf{A}}_k\hat{\mathbf{F}}_k|^2$ where $\hat{\mathbf{A}}_k$ is an accelerance row vector containing the transfer functions from the n force locations to the kth response location. By leaving out each response in turn and calculating the sum of squares of deviations, the averaged square deviation is calculated for that value of λ as

$$\Delta(\lambda) = \frac{1}{m}\sum_{k=1}^{m} |\hat{\mathbf{a}}_k - \hat{\mathbf{A}}_k\hat{\mathbf{F}}_k|^2. \tag{7}$$

The value of λ which gives smallest Δ is the optimum value of regularization parameter for that frequency.

2.3. Simulations

A simply supported rectangular steel plate of size $600 \times 500 \times 1.5\,\mathrm{mm}^3$ was used as a test structure in simulations that represent experiments, as in the earlier paper [11]. Four coherent point forces were applied perpendicular to the plate at randomly selected points. These forces were constant with respect to frequency when converted to one-third octave band form. Their values were 27, 19, 10 and 6 N. Five locations were chosen for operational response estimates and one location for the receiver response. Similar noise models as in Ref. [11] were used for corrupting the acceleration and force signals to represent the experimental situation. However, the amplitude of noise introduced here is higher than in Ref. [11] to enable better discrimination between the methods explored. Some bias errors, typically 30% of the response considered, are also added to the responses during the simulation.

In Ref. [11] it was observed that most of the methods performed reliably in the high-frequency region. For frequencies well below 500 Hz, where distinct modal behaviour is found, the force identification, and hence the response reconstruction, was more susceptible to errors and ill conditioning. In this paper therefore the simulations are concentrated on this part of the frequency range below 500 Hz. It is anticipated that this would not affect the final conclusions. The figures in one-third octave form from simulations show variations up to 400 Hz, which is the maximum centre frequency for the range considered.

Fig. 2 shows the identified forces obtained by Tikhonov regularization. The column at the right indicates the true force value, which should be the same at each one-third octave band. Figs. 3 and 4 show the equivalent results from singular value rejection based on accelerance error and the pseudo-inverse (over-determination), respectively. For singular value rejection a band of ± 1 S.D.

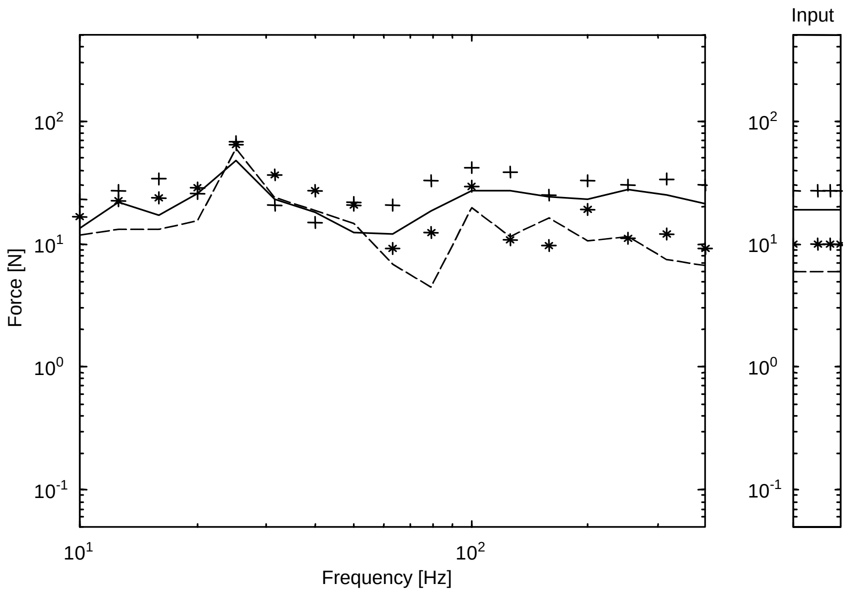

Fig. 2. Reconstructed forces in one-third octave bands by Tikhonov regularization for four sources and five responses: + + + , force 1; ——— , force 2; * * * , force 3; – – – , force 4.

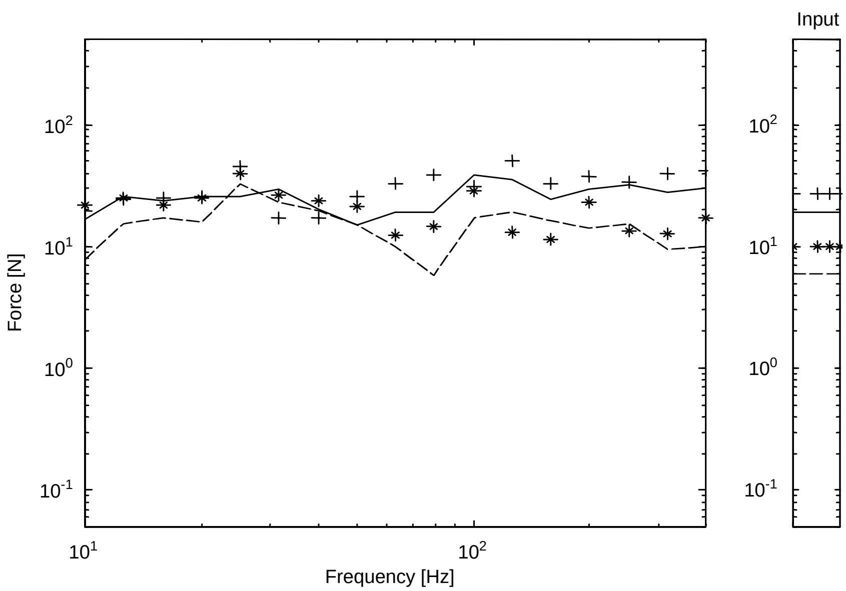

Fig. 3. Reconstructed forces in one-third octave bands with singular value rejection based on ± 1 S.D. for four sources and five responses: + + + , force 1; ——— , force 2; * * * , force 3; – – – , force 4.

is used in estimating the threshold as proposed in Ref. [11]. The force identification looks similar for Tikhonov and singular value rejection, except at the first resonance at 25 Hz, where the forces are identified more reliably by singular value rejection than by Tikhonov regularization. When

Table 1
Average one-third octave band errors in dB in simulation representing experiments to identify four forces from five responses

Method	Force 1 (27 N)	Force 2 (19 N)	Force 3 (10 N)	Force 4 (6 N)	Overall response
Moore–Penrose	7.2	8.9	14.3	17.5	4.9
Perturbation	2.9	4.9	8.9	14.4	4.4
SV rejection (based on accelerance errors)	2.7	3.5	6.4	8.2	3.4
Tikhonov-OCV	2.8	3.0	6.3	8.0	2.5
Iterative-CV	1.7	2.3	4.9	6.7	1.2

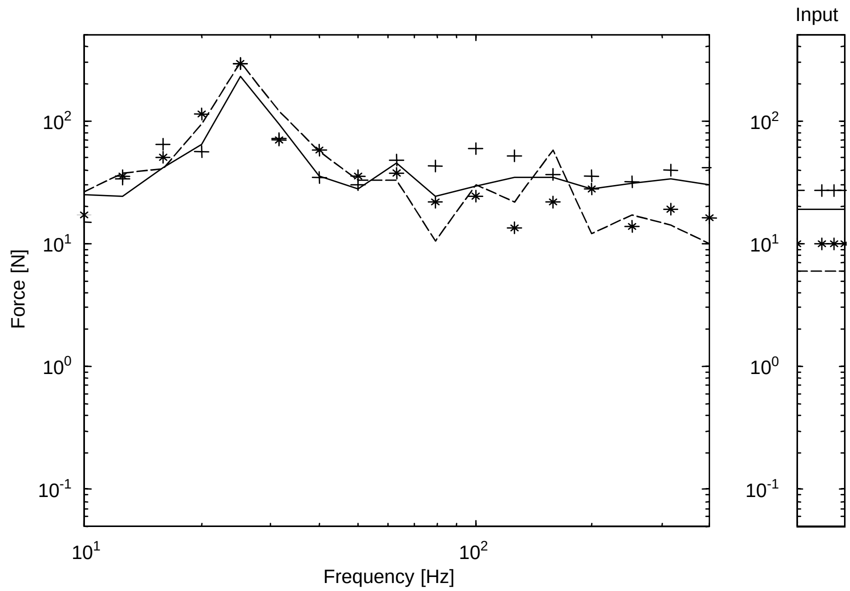

Fig. 4. Reconstructed forces in one-third octave bands using pseudo-inverse for four sources and five responses: + + + , force 1; ——— , force 2; * * * , force 3; – – – , force 4.

errors in the force estimation are quantified objectively the differences between methods become clearer. In fact the average error in the forces across all one-third octave bands is smallest for Tikhonov regularization. These errors are presented in Table 1, and are discussed more fully in Section 5, later in the paper. As expected, the errors were much larger for the pseudo-inverse, as seen from Fig. 4.

The velocity response at the receiver location predicted by Tikhonov regularization is shown in Fig. 5. The velocity prediction looks similar when using singular value rejection. The results of the two methods are compared in terms of a one-third octave band representation in Fig. 6. Once again, when the errors are quantified objectively over the whole frequency range, it is found that the Tikhonov regularization results in a smaller error than singular value rejection. The average velocity level errors over all bands are 3.4 and 2.5 dB for singular value rejection and Tikhonov

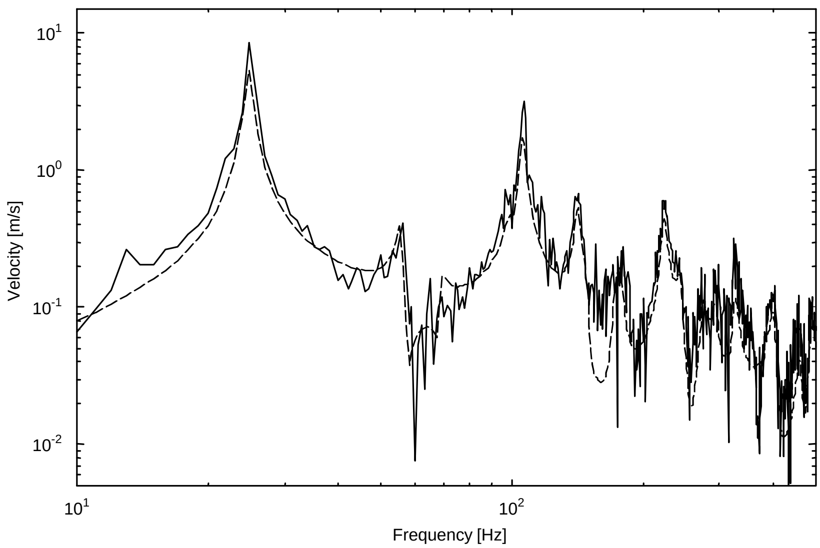

Fig. 5. Velocity response at the receiver location by Tikhonov regularization: ——— , predicted response; – – – , actual response.

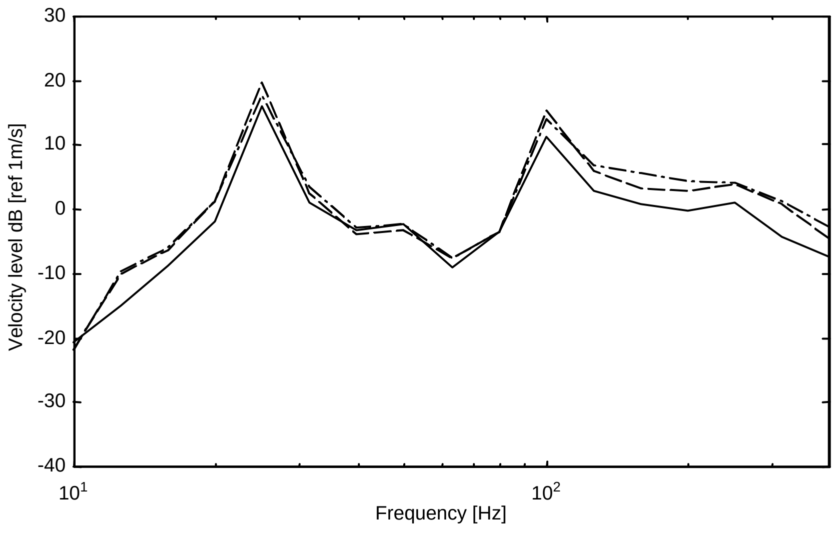

Fig. 6. One-third octave band velocity response by Tikhonov regularization: – – – , Tikhonov regularization; — · — , singular value rejection; ——— , actual response.

regularization, respectively. In addition, Tikhonov regularization is not expected to be sensitive to the level of errors in the responses and accelerances, as both errors are considered when selecting the regularization parameter using cross-validation. In general, Tikhonov regularization is found to be robust in force identification and response prediction compared with singular value rejection, since the latter was found to be sensitive to the level of error in the accelerances and responses, which can vary significantly [11].

3. Iterative inversion

3.1. Method

In this section an alternative method for regularization is considered, referred to as iterative inversion. The solution in this case is based on a formulation, such that when an infinite number of iterations is used, the solution tends to the Moore–Penrose pseudo-inverse. Errors in the force identification are again classified into two groups; bias error and variance around the mean. The bias error in the forces tends to zero as the number of iterations is increased, while the random error increases (see Fig. 1). By seeking a compromise in the bias error it is possible to limit the variance. In fact, there is an optimum number of iterations where the total error consisting of bias error and random error is minimized. This property of iterative inversion can be effectively utilized to reduce the combined error.

Iterative inversion [12] can be applied to force identification as follows. Given a kth estimate of the forces, $\hat{\mathbf{F}}_k$, the $(k+1)$th estimate is generated as

$$\hat{\mathbf{F}}_{k+1} = \beta\hat{\mathbf{A}}^{\mathrm{H}}\hat{\mathbf{a}} + (\mathbf{I} - \beta\hat{\mathbf{A}}^{\mathrm{H}}\hat{\mathbf{A}})\hat{\mathbf{F}}_k, \tag{8}$$

where the term added to $\hat{\mathbf{F}}_k$ is the difference between the reconstructed response $\hat{\mathbf{A}}\hat{\mathbf{F}}$ and the measured response $\hat{\mathbf{a}}$, which is multiplied by the convergence factor β and $\hat{\mathbf{A}}^{\mathrm{H}}$. Eq. (8) forms a geometric series with a geometric ratio of $\left(\mathbf{I} - \beta\hat{\mathbf{A}}^{\mathrm{H}}\hat{\mathbf{A}}\right)$. Therefore, the kth term can be written as

$$\hat{\mathbf{F}}_k = \beta(\mathbf{I} - (\mathbf{I} - \beta\hat{\mathbf{A}}^{\mathrm{H}}\hat{\mathbf{A}}))^{-1}(\mathbf{I} - (\mathbf{I} - \beta\hat{\mathbf{A}}^{\mathrm{H}}\hat{\mathbf{A}})^{k+1})\hat{\mathbf{A}}^{\mathrm{H}}\hat{\mathbf{a}}. \tag{9}$$

Using singular value decomposition of the accelerance matrix, $\hat{\mathbf{A}} = \mathbf{USV}^{\mathrm{H}}$ with $\mathbf{S} = \mathrm{diag}(s_i)$ and after some simplification, Eq. (9) can be written as

$$\hat{\mathbf{F}}_k = \mathbf{V}\left[\mathrm{diag}\left(\frac{1-(1-\beta s_1^2)^{k+1}}{s_1}, \ldots, \frac{1-(1-\beta s_n^2)^{k+1}}{s_n}\right)\middle|[\mathbf{0}]_{n\times(m-n)}\right]\mathbf{U}^{\mathrm{H}}\hat{\mathbf{a}}. \tag{10}$$

Details of the above derivations are given in Ref. [12].

3.2. Optimum iteration number

To find the optimum number of iterations in order to minimize the combined error it is necessary to formulate an expression to estimate the bias error and the variance. The expressions can be derived following Ref. [16]. If it is assumed that the standard deviation on all measurement channels has a common value, the mean square error, which consists of bias error and variance, is given by

$$\varepsilon_k^2 = \sigma^2\left(2\sum_{i=1}^{n}\phi_i - n\right) + \hat{\mathbf{b}}^{\mathrm{H}}\hat{\mathbf{b}} \tag{11}$$

where $\phi_i = 1-(1-\beta s_i^2)^{k+1}$, n is the rank of the accelerance matrix, $\hat{\mathbf{b}} = (\boldsymbol{\delta}_k - \mathbf{I})\hat{\mathbf{a}}$ is the bias error, and σ is the standard deviation in the response measurements. The iteration number k which results in the minimum mean squared error is the optimum iteration number that gives the best compromise between bias error and the magnified random errors. When the standard deviation in the response measurements is different for each channel, Eq. (11) takes the form [20]

$$\varepsilon_k^2 = \mathrm{trace}(\boldsymbol{\delta}_k\,\mathbf{COV}(\mathbf{a})\boldsymbol{\delta}_k^{\mathrm{H}}) + \mathrm{trace}\{(\boldsymbol{\delta}_k - \mathbf{I})\mathbf{COV}(\mathbf{a})(\boldsymbol{\delta}_k - \mathbf{I})^{\mathrm{H}}\} - \hat{\mathbf{b}}^{\mathrm{H}}\hat{\mathbf{b}}, \tag{12}$$

where $\boldsymbol{\delta}_k = \mathbf{U}\,\mathrm{diag}(\phi_1, \ldots, \phi_n, 0_{n+1}, \ldots, 0_m)\mathbf{U}^{\mathrm{H}}$ and $\mathbf{COV}(\mathbf{a})$ signifies $(\hat{\mathbf{a}} - \mathbf{AF})(\hat{\mathbf{a}} - \mathbf{AF})^{\mathrm{H}}$.

3.3. Convergence

The convergence parameter β determines how fast the iterative inverse converges to the Moore–Penrose pseudo-inverse. The larger the value of convergence parameter, the faster is the convergence. However, for convergence to occur the following condition has to be satisfied:

$$(\mathbf{I} - \beta\hat{\mathbf{A}}^{\mathrm{H}}\hat{\mathbf{A}})^{k+1} \to [0] \quad \text{as} \quad k \to \infty. \tag{13}$$

The above expression sets an upper limit for the convergence parameter. Using singular value decomposition, this convergence criterion can also be written as $(1 - \beta s_i^2) < 1$ for $i = 1, 2, \ldots, n$. Therefore $\beta < 1/s_i^2$.

If a common convergence parameter value β is used for all singular values, as implied in the above, the part of the solution contributed by the larger singular values converges faster than that relating to the smaller ones. The difference increases as the condition number increases. Since in the case of a high condition number, smaller singular values are prone to modification by measurement errors, the slower convergence can be effectively utilized in restricting the iteration to reduce the error propagation. To accommodate the above criterion, the convergence parameter can be written as $\beta = c/s_1^2$ where c is a constant less than one.

3.4. Cross-validation concept

The standard deviation in the operational response used in Eqs. (11) or (12) can be obtained either directly (during averaging of multiple samples) or indirectly as in Ref. [21]. Based on this standard deviation, the cut-off iteration number can be determined. There is a difficulty in choosing the cut-off iteration number by this means when the standard deviation is larger than or considerable in magnitude compared to the response itself (e.g., at antiresonance). In this situation, based on the error expression it is observed that the cut-off criterion is already satisfied at the first iteration. This results in an underestimation of the forces concerned. Another problem is faced at resonance where the standard deviation is very small compared with the operational response which might lead to a large number of iterations being required to reach a minimum total error. A large number of iterations means larger amplification of measurement errors. Hence, the force reconstruction would be incorrect in both cases.

These problems can be overcome if a fixed percentage of the operational response at each frequency is taken as the assumed standard deviation (e.g., 10% or 20% of the response). This might introduce a bias in the response predicted at the receiver location depending on what fixed percentage of the response is used as the standard deviation (large values introduce large bias). The fraction of the operational response to be used as the assumed standard deviation can be treated as a variable. In this study a method of cross-validation is proposed in which the reconstructed forces are used to derive operational responses other than the ones used for force reconstruction. For this, the fraction is varied in some range (10–50%) in small steps (5% step). For each step, the validation error is derived as

$$VE = \sum_{j=1}^{m} \frac{||\tilde{\mathbf{a}}_{valid}|_j - |\hat{\mathbf{a}}_{valid}|_j|}{|\hat{\mathbf{a}}_{valid}|_j}, \tag{14}$$

where m is number of validating responses used, $\tilde{\mathbf{a}}_{valid}$ is a vector of reconstructed validating operational responses and $\hat{\mathbf{a}}_{valid}$ is a vector of measured validating operational responses. The fraction which results in the smallest validation error at each frequency is used for force reconstruction at those frequencies as the assumed standard deviation of the response.

3.5. Simulations

Fig. 7 shows the forces identified by iterative inversion using the above cross-validation concept. Except at the first resonance, the forces are identified reliably compared with both Tikhonov regularization and singular value rejection based on accelerance error (compare Fig. 7 with Figs. 2 and 3). The forces are predicted more reliably at higher frequencies than at lower frequencies, with individual forces overestimated in the low-frequency region. Fig. 8 shows the velocity response predicted at the receiver location. This is also considerably better than that obtained using Tikhonov regularization or singular value rejection (compare Figs. 8 and 5). A similar trend is observed in the one-third octave band representation (Fig. 9).

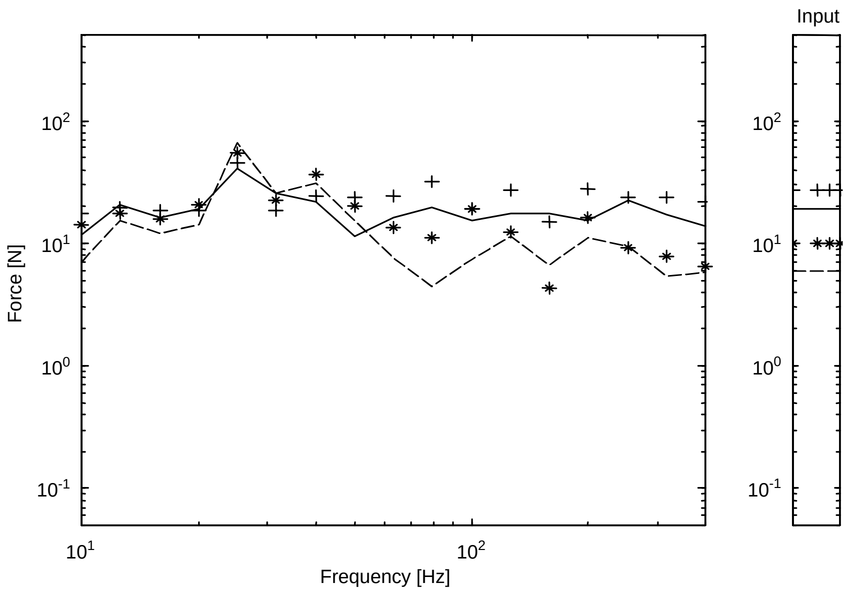

Fig. 7. Reconstructed forces in one-third octave bands by iterative inversion with standard deviation taken as fixed percentage (up to 50%) of responses using cross-validation: + + + , force 1; ——— , force 2; * * * , force 3; – – – , force 4.

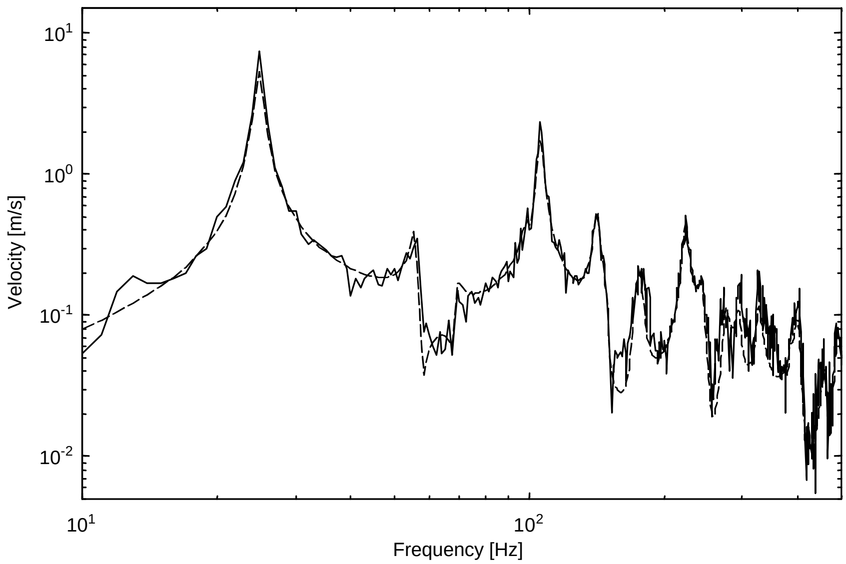

Fig. 8. Velocity response at the receiver location by Iterative inversion with standard deviation taken as fixed percentage (up to 50%) of responses using cross-validation: – – – , predicted response; ——— , actual response.

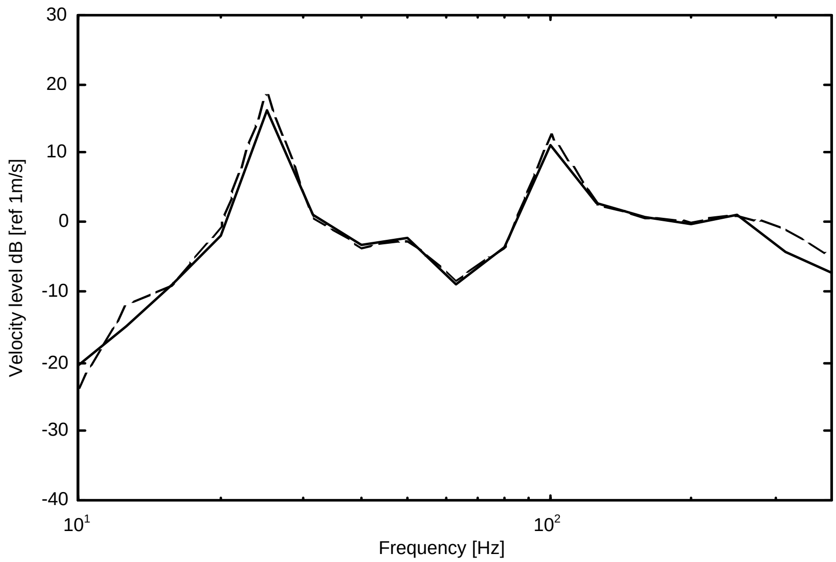

Fig. 9. One-third octave band velocity response at the receiver location—iterative inversion with standard deviation taken as fixed percentage (up to 50%) of responses using cross-validation: ——— , predicted response; – – – , actual response.

4. Experimental validation

As well as the simulations described above, experimental validation of the techniques has been performed. The same experimental set-up as in Ref. [11] has been used. This consisted of a flat

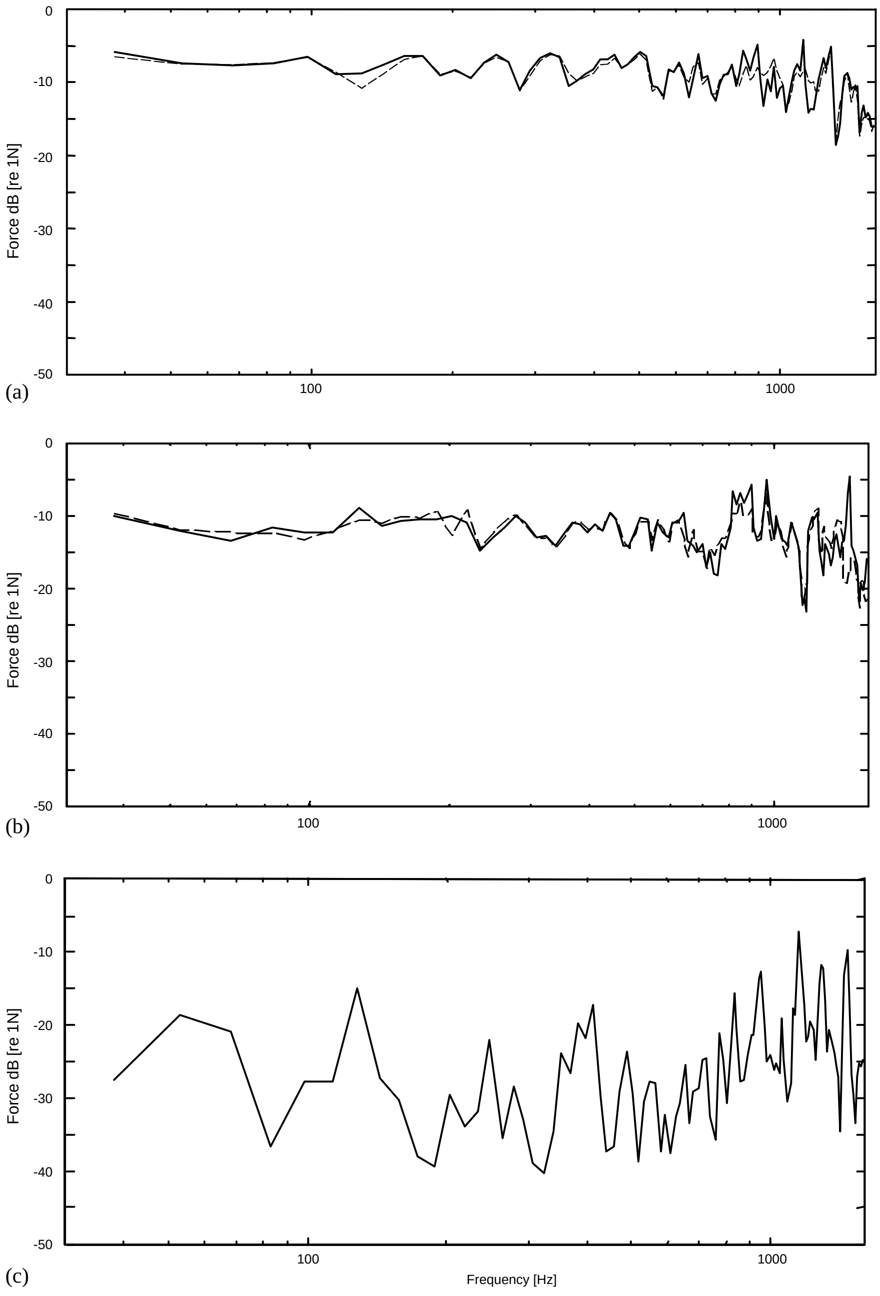

Fig. 10. Identified forces from measurements in constant 15 Hz bands by Tikhonov regularization: (a) force 1; (b) force 2; and (c) force 3. ——— , force identified; – – – , actual force.

rectangular plate ($700 \times 500 \times 1.5\,\text{mm}^3$) made of steel, hung from a frame using elastic threads. Two simultaneous forces were applied to the plate using electrodynamic shakers. A third force position, force 3, is included in the experiment but is actually 0 during the operational response measurements. This ensures that the matrices are of realistic size without adding unnecessary complication to the experiment. The shakers were connected to the plate through force gauges. Accelerometers and force gauges were mounted on cementing studs, which were glued to the plate. A frequency range of 30–1600 Hz was used in the analysis with a frequency resolution of 1 Hz. The measurements performed consist of operational responses measured at a series of locations on the plate when both shakers were in operation (this represents a situation where some machine is mounted on the plate), and frequency response functions from each of the three forcing locations to response locations. Four locations are used as operational responses and a fifth as the receiver location to be compared with predictions.

The forces identified by Tikhonov regularization are shown in Figs. 10a–c averaged into constant frequency bands of 15 Hz. The Tikhonov regularization, along with ordinary cross-validation for the selection of the regularization parameter, results in good force identification at low frequencies. Force 1 is very well predicted by this method (as it is a largest force, relative errors are smallest). Force 3, which is the smallest force (actually zero), is poorly estimated. The velocity predicted by this method is shown in Fig. 11. It is predicted accurately in the low-frequency region, but some errors are observed in the high-frequency region between 800 and 1600 Hz.

Fig. 12 shows the forces derived using iterative inversion with cross-validation, allowing a variable percentage of the response at each frequency as the standard deviation. This results in similar estimates for the forces as from Tikhonov regularization (compare Fig. 12 with Fig. 10).

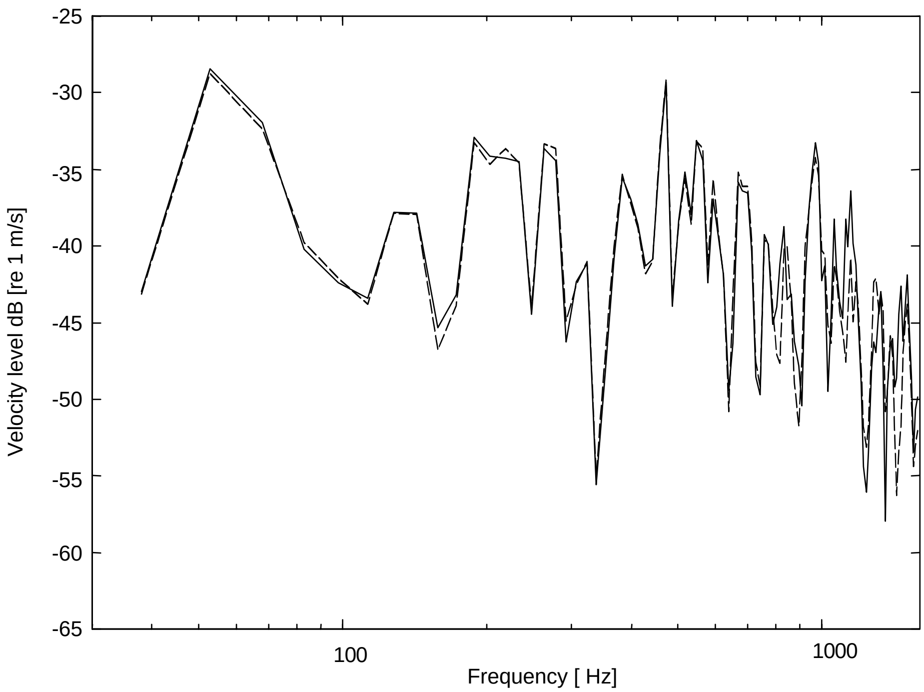

Fig. 11. Predicted overall response from measurements in constant 15 Hz frequency bands by Tikhonov regularization: ——— , predicted response; – – – , actual response.

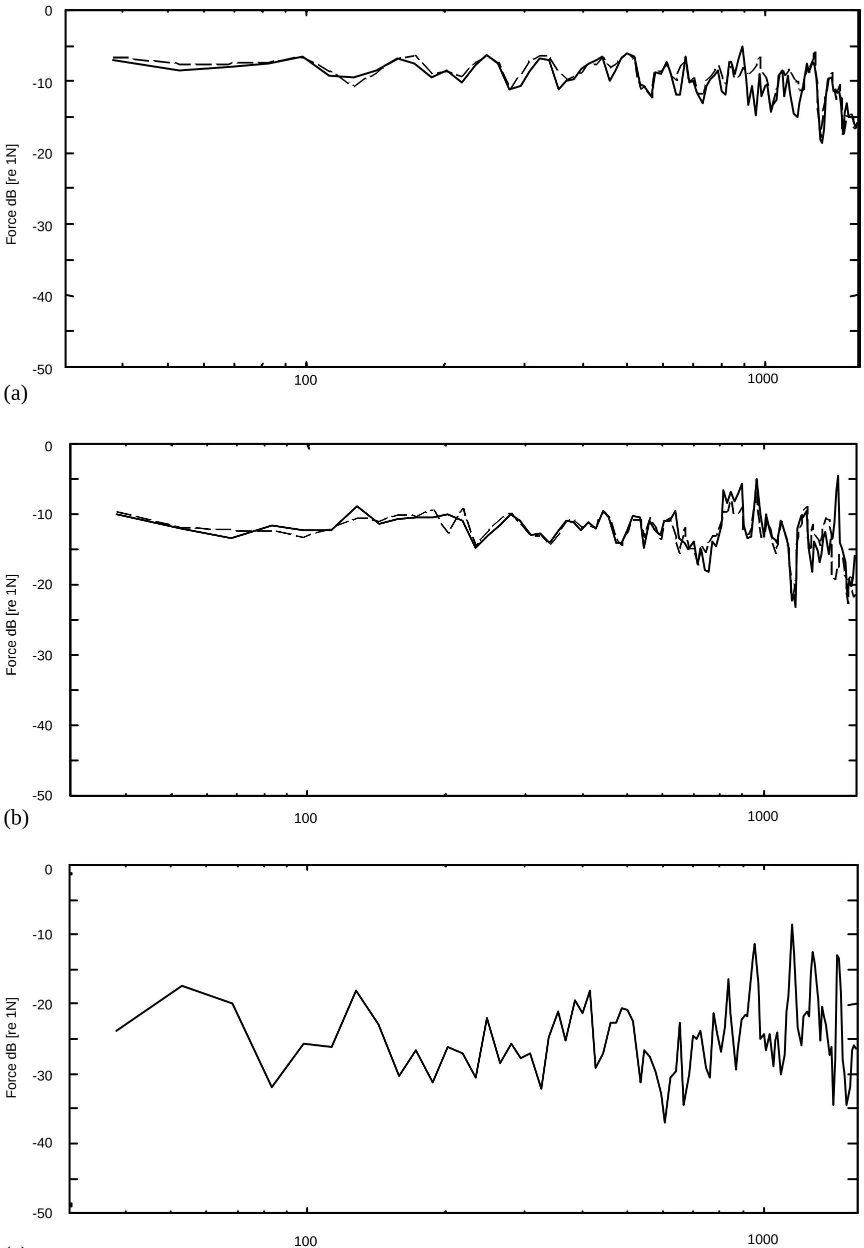

Fig. 12. Identified forces from measurements in constant 15 Hz bands by iterative inversion with cross-validation: (a) force 1; (b) force 2; and (c) force 3. ——— , force identified; – – – , actual force.

Some spikes are reduced in magnitude in the frequency range 1000 to 1600 Hz. This method, however, results in underestimation of some forces and hence the mean force errors over all bands are increased compared to Tikhonov regularization. The overall response (Fig. 13) is predicted marginally better than that from Tikhonov regularization in the frequency range 1000–1600 Hz

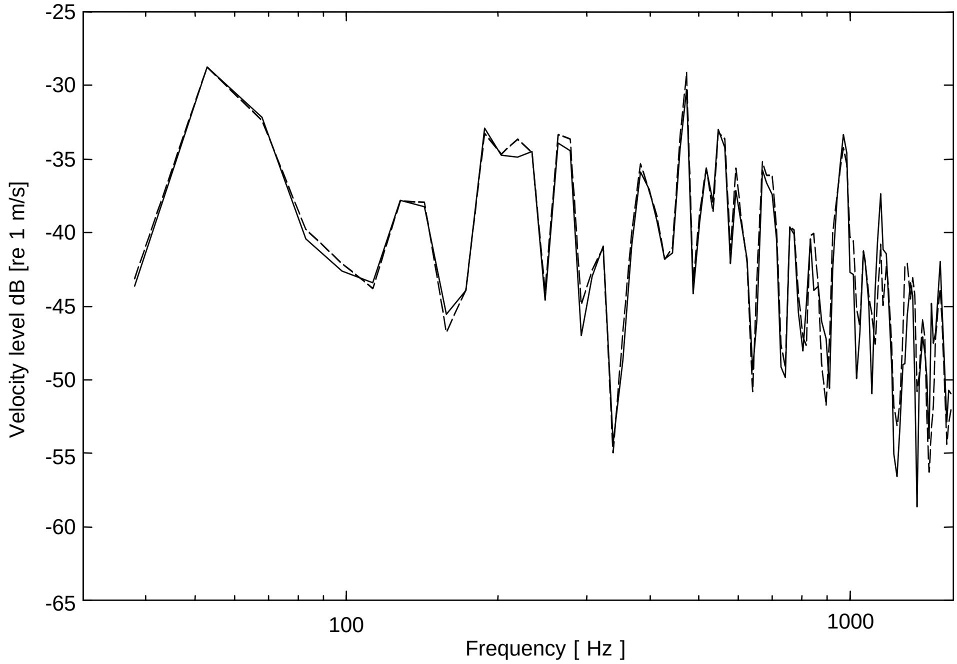

Fig. 13. Predicted overall response from measurements in constant 15 Hz by iterative inversion with cross-validation: ——— , predicted response; – – – , actual response.

(compare with Fig. 11). In the calculations the standard deviation is allowed to vary between 5% and 75% of the response in steps of 5%.

5. Discussion

The results for all the methods considered here and in Ref. [11] are summarized in Table 1 for the simulations. In all cases in the simulations, the error levels are as used in this paper, which are higher than considered in Ref. [11]. The results from the simulations are the root mean square differences between measured and predicted levels, taken across all one-third octave bands from 10 to 400 Hz. These results indicate the superiority of both iterative inversion and Tikhonov regularization over all other methods used, with iterative inversion giving the best results.

Table 2 gives equivalent results from the experiment and is based on one-third octave bands over the whole range of 31.5–1600 Hz. The errors from the experimental study are also calculated using a constant bandwidth representation (15 Hz bands between 30 and 1600 Hz) as this allows greater discrimination between the methods. These are shown in Table 3. In Tables 2 and 3, the errors from the experimental force identification are obtained for forces 1 and 2 by comparing the results with the respective measured forces in the various bands between 30 and 1600 Hz. The numbers indicated are root mean square dB level errors and should be small for good force identification. Since force 3 is zero, the 'error' in the reconstruction is obtained by comparing it

Table 2
Summary of errors in dB, averaged over all one-third octave frequency bands from experimental force identification by different techniques to identify three forces from four responses

Method	Force errors			Response errors			
	*F*1	*F*2	*F*3	*Overall*	Contribution from force 1	Contribution from force 2	Contribution from force 3
Moore–Penrose	1.3	1.5	20.3	**1.5**	1.3	1.5	23.3
Perturbation	0.6	0.9	17.3	**0.5**	0.8	1.0	21.0
SV rej (accelerance)	1.7	1.9	19.1	**1.5**	1.6	2.2	21.7
SV rej (response)	4.5	3.5	11.0	**3.0**	4.8	3.6	13.0
Tikhonov-OCV	0.5	0.7	18.4	**0.5**	0.8	0.8	22.4
Iterative-CV	0.7	0.9	15.2	**0.7**	1.2	0.9	18.1

*F*1 and *F*2 indicate root mean square dB level errors compared to measured forces 1 and 2 while *F*3 indicates dB level difference between identified force 3 and maximum measured force level in corresponding frequency bands. Similarly response errors are root mean square dB level errors compared to measured responses. The contribution from force 3 is compared with the overall response.

Table 3
Summary of errors in dB, averaged over all 15 Hz frequency bands from experimental force identification by different techniques to identify three forces from four responses

Method	Force errors			Response errors			
	*F*1	*F*2	*F*3	*Overall*	Contribution from force 1	Contribution from force 2	Contribution from force 3
Moore–Penrose	1.9	2.9	18.9	**3.0**	2.1	3.0	22.0
Perturbation	1.5	2.8	17.2	**2.8**	1.6	2.9	20.2
SV rej (accelerance)	1.9	2.9	18.9	**3.0**	2.1	3.0	22.0
SV rej (response)	4.0	3.3	12.9	**3.9**	4.0	3.7	16.3
Tikhonov-OCV	1.5	2.6	18.3	**2.6**	1.6	2.6	21.3
Iterative-CV	1.7	2.3	15.5	**2.3**	1.8	2.4	18.9

*F*1 and *F*2 indicate root mean square dB level errors compared to measured forces 1 and 2 while *F*3 indicates dB level difference between identified force 3 and maximum measured force level in corresponding frequency bands. Similarly response errors are root mean square dB level errors compared to measured responses. The contribution from force 3 is compared with the overall response.

with the maximum dB level of the other two forces in the frequency band. This number should therefore be as high as possible to indicate a good prediction. Similarly, the errors in force contributions 1 and 2 are obtained by comparing the results with those calculated using measured forces and the accelerance matrix. The error in the overall response is the root mean square dB level error from the measured response at the receiver location. The contribution from force 3 should be zero, so its predicted contribution is compared with the total response. This number should again be as large as possible to indicate a good prediction. From Tables 2 and 3 it can be seen that Tikhonov regularization and iterative inversion with cross-validation produce equally good force reconstruction and response prediction, both being better than other methods. Table 2 suggests that the perturbation method [11] is equally good although from Table 3 it can be seen that this is slightly worse in these results.

Iterative inversion with cross-validation performed better than Tikhonov regularization with ordinary cross-validation in the simulations but was similar in the measurements. This was found to be due to the large amount of noise introduced in the operational responses during the simulations. In this situation, the Tikhonov regularization parameter selection by ordinary cross-validation is not wholly reliable. Although iterative inversion with cross-validation also depends on the accuracy of the measured responses, by assuming a non-zero minimum standard deviation (in simulations 5%) better predictions are observed.

6. Conclusions

Using both simulations on a simply supported rectangular flat steel plate and measurements on hanging rectangular flat plate it has been shown that the determination of forces by inverse methods can be improved by various techniques. Tikhonov regularization, using ordinary cross-validation to select the regularization parameter, is found to identify the forces much better than all the methods previously investigated. However, this method does not reduce the error magnification in certain cases because of the way the regularization parameter is varied (0–50% of maximum singular value). It seems advisable to set a non-zero minimum value for the regularization parameter based on the error in either the response or the accelerance. Both Tikhonov regularization and iterative inversion methods result in better identification of individual forces and their contribution compared with the singular value rejection or perturbation of the accelerance matrix. Iterative inversion combined with a validation technique is found to be the most robust of all the methods investigated in terms of the response prediction. In arriving at the best-fit response prediction, however, this method results in underestimation of some forces at many frequencies. Hence the individual contributions might contain larger errors. It also takes about 7 times longer to calculate the inverse using this method than by Tikhonov regularization.

As in Ref. [11], it is recognized that the conclusions of the work here are based on a study of only one type of structure. By covering a wide frequency range the study has covered both low and high modal density regions. There should be no restriction on the use of the techniques studied here for more general built-up structures, provided that sufficient excitation and response positions are selected.

References

[1] LMS Application Notes on Transfer Path Analysis, The Qualification and Quantification of Vibro-acoustic Transfer Paths, LMS International, Leuven, Belgium, 1995.

[2] P. Mas, P. Sas, K. Wyckaert, W. Hendrickx, P. Van Der Linden, Noise and vibration transfer path analysis, Proceedings International Seminar on Applied Acoustics ISAAC 6, Vol. IV, Leuven, 1995, pp. 1–22.

[3] U. Fingberg, T. Ahlersmeyer, Noise path analysis of structure-borne engine excitation to interior noise of a vehicle, Proceedings of the 17th International Seminar on Modal Analysis, Leuven, Belgium, 1992, pp. 143–152.

[4] J. Romano, J.A., Lopez, Practical application of transfer path analysis to resolve structure-borne noise problems in vehicle design, Proceedings of the 21st International Seminar on Modal Analysis, Leuven, Belgium, 1996, pp. 527–536.
[5] M.H.A. Janssens, J.W. Verheij, D.J. Thompson, The use of an equivalent forces method for the experimental quantification of structural sound transmission, Journal of Sound and Vibration 226 (1999) 305–328.
[6] J.W. Verheij, Inverse and reciprocity methods for machinery noise source charectrization and sound path quantification, Part 1: sources, International Journal of Acoustics and Vibration 2 (1) (1997) 11–20.
[7] J.W. Verheij, Inverse and reciprocity methods for machinery noise source characterization and sound path quantification, Part 2: transmission paths, International Journal of Acoustics and Vibration 2 (3) (1997) 103–112.
[8] M.H.A. Janssens, J.W. Verheij, T. Loyau, Experimental example of the pseudo-forces method used in characterisation of a structure-borne sound source, Applied Acoustics 63 (1) (2002) 9–34.
[9] A.N. Thite, D.J. Thompson, Study of indirect force determination and transfer path analysis using numerical simulations for a flat plate, ISVR Technical Memorandum No. 851, May 2000.
[10] J.A. Fabunmi, Effects of structural modes on vibratory force determination by pseudo-inverse technique, American Institute of Aeronautics and Astronautics Journal 24 (3) (1986) 504–509.
[11] A.N. Thite, D.J. Thompson, The quantification of structure-borne transmission paths by inverse methods. Part 1: Improved singular value rejection methods, Journal of Sound and Vibration 264 (2003) 411–431, this issue.
[12] J. Biemond, R.L. Lagendijk, R.M. Mersereau, Iterative methods for image processing, Proceedings of the IEEE 78 (5) (1990) 856–883.
[13] P.A. Nelson, Some inverse problems in acoustics, Sixth International Congress on Sound and Vibration, 5–8 July 1999, Lyngby, Denmark, 1999, pp. 7–32.
[14] P.A. Nelson, S.H. Yoon, Estimation of acoustic source strength by inverse methods, Part 1: conditioning of the inverse problem, Journal of Sound and Vibration 233 (4) (2000) 643–668.
[15] S.H. Yoon, P.A. Nelson, Estimation of acoustic source strength by inverse methods, Part II: experimental investigation of methods for choosing regularization parameters, Journal of Sound and Vibration 233 (4) (2000) 669–705.
[16] B.K. Kim, J.G. Ih, Design of an optimal wave vector filter for enhancing the resolution of reconstructed source field by near-field acoustical holography (NAH), Journal of Acoustical Society of America 107 (6) (2000) 3289–3297.
[17] P.A. Nelson, S.J. Elliott, Active Control of Sound, Academic Press, London, 1992, pp. 416–420.
[18] A. Tikhonov, V. Arsenin, Solution of Ill-Posed Problems, Winston, Washington, DC, 1977.
[19] D.M. Allen, The relationship between variable selection and data augmentation and a method for prediction, Technometrics 16 (1974) 125–127.
[20] A.N. Thite, D.J. Thompson, Study of regularized solutions to improve the indirect force determination and transfer path analysis using numerical simulations for a flat plate, ISVR Technical Memorandum No. 855, 2000.
[21] J.L. Bendat, A.G. Piersol, Engineering Application of Correlation and Spectral Analysis, 2nd Edition, Wiley Interscience, New York, 1993.